



# Generation of 3D lung organoids from human induced pluripotent stem cells for modeling of lung development and viral infection

Shashi Kant Tiwari, Tariq M. Rana <sup>\*,1</sup>

Division of Genetics, Department of Pediatrics, Program in Immunology, Institute for Genomic Medicine, University of California San Diego, 9500 Gilman Drive MC 0762, La Jolla, CA, 92093, USA

## ARTICLE INFO

### Keywords:

Lung organoids  
Human iPS cells  
SARS infection  
Lung development

## ABSTRACT

The lack of physiologically relevant *in vitro* models has hampered progress in understanding human lung development and disease. Here, we describe a protocol in which human induced pluripotent stem cells (hiPSCs) undergo stepwise differentiation into definitive endoderm (>88% population) to three-dimensional (3D) lung organoids (LORGs), which contain both epithelial and mesenchymal cellular architecture and display proximal and distal airway patterning. These LORGs can be maintained for more than 90 days by re-embedding in the Matrigel. We show the utility of LORGs for disease modeling and drug screening by infection with severe acute respiratory syndrome coronavirus 2 (SARS-CoV-2) and treatment with antiviral drugs.

## 1. Maintenance and passaging of hiPSCs

### 1.1. Timing: 45–90 min

For complete details on the use and execution of this protocol, please refer to Ref. [1].

Proper maintenance of hiPSCs in culture is essential to the success of the LORG differentiation protocol. In our hands, the optimal conditions for the maintenance of undifferentiated hiPSCs are culture in mTeSR1 medium containing Y-27632 (10  $\mu$ M) in 6-well tissue culture plates coated with growth factor-reduced Matrigel basement membrane (GFR-M, 100  $\mu$ g/mL, Cat No. 354230) at 37 °C in a humidified 5% CO<sub>2</sub> incubator. Y-27632, a Rho-associated kinase (ROCK) inhibitor, is added to the medium to enhance the recovery of iPSC cells from cryopreserved stocks and increases the number of colonies and colony size. For propagation, hiPSCs from the 6-well plates, 70–80% confluent, are then split 1:6 into fresh 6-well or 24-well plates as described here.

**CRITICAL:** Too low confluency may result in an insufficient cell yield after DE differentiation, while too high confluency may result in incomplete differentiation into DE.

1. Thaw the GFR-M stock on ice until it completely melts and dilute it to 100  $\mu$ g/mL in cold DMEM/F12 medium and add 1mL/well of diluted Matrigel to a 6-well plate. Leave at 37 °C for 1 h to coat the wells.

**CRITICAL:** Matrigel solidifies at room temperature. Therefore, keep small aliquots of the stock at –20 °C and thaw on ice

\* Corresponding author.

E-mail address: [trana@ucsd.edu](mailto:trana@ucsd.edu) (T.M. Rana).

<sup>1</sup> Lead contact.

<https://doi.org/10.1016/j.heliyon.2023.e19601>

Received 15 February 2023; Received in revised form 20 August 2023; Accepted 28 August 2023

Available online 29 August 2023

2405-8440/© 2023 The Authors. Published by Elsevier Ltd. This is an open access article under the CC BY-NC-ND license (<http://creativecommons.org/licenses/by-nc-nd/4.0/>).

immediately before use.

2. Prewarm DMEM/F12, mTeSR1, and either dispase (1 mg/mL) or Versene (1 mg/mL) in a 37 °C water bath for ~15 min.
3. Aspirate the culture medium from the hiPSC cultures, add 1 mL dispase or Versene solution to each well, and incubate for 5–10 min in a 37 °C incubator. Observe the cells under a light microscope to check for evidence that the colonies are beginning to detach from the tissue culture plate.
4. Carefully aspirate the dispase/Versene reagent and gently wash (2–3 times) the still-attached colonies with prewarmed DMEM/F12.
5. Add Y-27632 to the prewarmed mTeSR1 medium at a final concentration of 10 μM. Prepare tubes containing 4.5 mL of this medium (one tube per well). Using a cell scraper, gently scrape the hiPSCs from the culture plate and then transfer cells with remaining culture medium into tubes with a pipette and triturate the colonies into small aggregates using a 5 mL serological pipette.
6. Take the 6- or 24-well plates containing GFR-M (step 1), aspirate the GFR-M, and add 0.5 mL/well of the triturated hiPSCs to 6-well or 24-well plates. For the 6-well plates only, add an additional 1.5 mL/well of the prewarmed mTeSR1/Y-27632 medium.
7. Gently shake the plates in a side-to-side motion to evenly distribute the hiPSCs across the wells and place in a 37 °C 5% CO<sub>2</sub> incubator.

**CRITICAL:** hiPSCs must be evenly distributed across the well to ensure optimal colony growth before dissociation and seeding into differentiation cultures (see Troubleshooting Problem 1, Fig. 1A and B).

#### Key resources table

REAGENT	SOURCE	IDENTIFIER
<b>Antibodies</b>		
Mouse anti-FOXP1	eBioscience	14-9965-82
Mouse anti-surfactant protein B (SFTPB)	Seven Hills Bioreagents	Wmab-1B9
Rabbit anti-prosurfactant protein C (proSP-C)	Millipore	AB3786
Rabbit anti-RAGE	Abcam	ab216329
Mouse anti-Hop (E-1)	Santa Cruz	Sc-398703
Rabbit anti-NKX2.1	Abcam	ab76013
Rabbit anti-SOX9	Millipore	AB5535
Rabbit anti-ECAD	Cell Signaling Technology	3195
Mouse anti-CC10 (SCGB1A1)	Santa Cruz	sc-365992
Rabbit Anti-ACE2	Novus Biologicals	NBP2-67692
Rabbit anti-TMPRSS2	Abcam	ab92323
Rabbit anti-Ki67	Millipore	AB9260
Mouse anti-GFAP	Sigma-Aldrich	G3893
Rabbit anti-SOX2	Abcam	ab97959
Mouse anti-β-tubulin III	Abcam	ab7751-100
Chicken anti-Nestin	Abcam	ab134017
Chicken anti-MAP2	Abcam	ab5392
Alexa Fluor 488, 594, and 647 conjugated secondary antibodies	Molecular Probes/Invitrogen	A11032, A11034, A11012, A11039, A11001
Antifade mounting medium with DAPI (Vectashield)	Vector Laboratories	H-1200

(continued on next page)

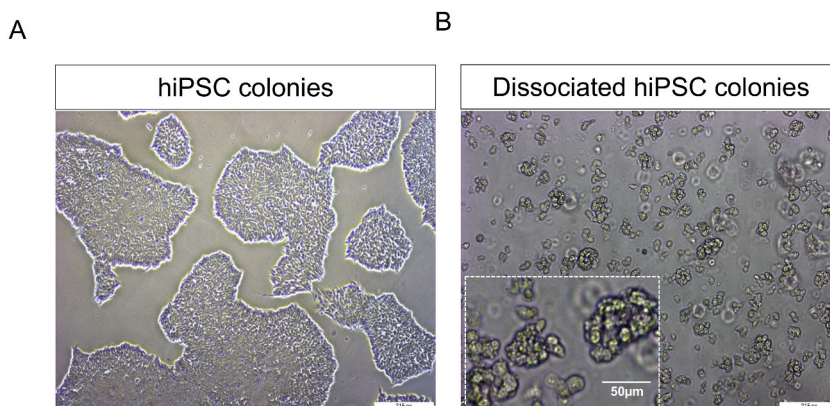


**Fig. 1.** hiPSC culture and seeding for differentiation.

(A) Representative phase contrast image of a hiPSC culture showing healthy colonies with optimal confluency before seeding. Scale bar, 200 μm. (B) Representative light microscopic image showing the optimal size of dissociated hiPSC colonies for seeding and differentiation. Scale bar, 200 μm. Inset magnification = 50 μm.

(continued)

REAGENT	SOURCE	IDENTIFIER
<b>Chemicals</b>		
1-Thioglycerol	Sigma-Aldrich	M6145
L-Ascorbic acid	Tocris Bioscience	4055
Bovine serum albumin (BSA)	Fisher Scientific	BP9703-100
Protease and phosphatase inhibitor cocktail	Pierce	A32955
Bio-Rad DC protein assay kit	Bio-Rad	5000112
Chemiluminescence substrate	Thermo Scientific	34580
Optimal cutting temperature (OCT) compound	Tissue-Tech	4583
RIPA buffer	Teknova	R3792
Falcon™ Cell Culture Inserts	BD, Falcon	08-770
β-Mercaptoethanol	Sigma-Aldrich	M7522
Immun-Blot PVDF membrane	Bio-Rad Laboratories	1620177
<b>Growth Factors</b>		
Activin A	R&D Systems	338-AC
FGF10 (recombinant human fibroblast growth factor 10)	R&D Systems	345-FG
FGF4 (recombinant human fibroblast growth factor 4)	R&D Systems	7460-F4
FGF7 (recombinant human fibroblast growth factor 7)	R&D Systems	251-KG/CF
NOGGIN	R&D Systems	6057
Smoothed agonist (SAG)	Enzo Life Sciences	ALX-270-426-M001
Epidermal growth factor (EGF)	Sigma-Aldrich	E9644
Basic fibroblast growth factor (bFGF)	Sigma-Aldrich	F0291
<b>Small molecules</b>		
SB431542 (selective inhibitor of the transforming growth factor-β (TGF-β) type I receptor)	TOCRIS	1614
CHIR9902 (GSK3β inhibitor/Wnt activator)	TOCRIS	4423
Y-27632 (ROCK inhibitor)	Sigma-Aldrich	SCM075
<b>Cell Lines</b>		
Human induced pluripotent stem cells (hiPSCs)	Cell Application	hiPS11-10
293FT (HEK)	American Type Culture Collection (ATCC)	CRL-1573
Calu-3 human lung epithelial cell	ATCC	HTB-55
<b>Culture Media</b>		
Advanced DMEM	Thermo Fisher Scientific	12491015
CHIR99021	Stem cell Technologies	72054
GlutaMAX (100X)	Thermo Fisher Scientific	35050061
HEPES (1 M)	Thermo Fisher Scientific	15630080
mTeSR	Stem cell Technologies	85850
N-2 supplement	Thermo Fisher Scientific	17502048
Penicillin-streptomycin (100X)	Thermo Fisher Scientific	15140122
RPMI 1640 medium	Thermo Fisher Scientific	11875119
Matrigel basement membrane matrix (growth factor reduced)	Corning	354230
Matrigel basement membrane matrix	Corning	354234
Versene solution	Thermo Fisher Scientific	15040066
DMEM/F12	Thermo Fisher Scientific	11320082
MEM nonessential amino acids (MEM-NEAA)	Thermo Fisher Scientific	11140050
B-27 supplement without ATRA	Thermo Fisher Scientific	12587010
B-27 supplement with ATRA	Thermo Fisher Scientific	17504044
GlutaMAX, 200 mM	Thermo Fisher Scientific	35050061
L-Glutamine	Thermo Fisher Scientific	A2916801
Dispase	Thermo Fisher Scientific	17105-0412q
Collagenase IV	Thermo Fisher Scientific	17104019
Fetal bovine serum (FBS)	Thermo Fisher Scientific	10438-018
Bovine serum albumin (BSA)	Fisher Scientific	BP9703-100

## 1.2. Materials and equipment

## 2. Step-by-step method details

**Note:** All procedures for differentiation of hiPSCs into DE, AFE, and 3D LORGs are adapted from Refs. [2,3].

### 3. DE induction (Days 1–4)

#### 3.1. Timing: 4 days

In the first step, hiPSCs are induced to differentiate into DE. Physiologically, this germ layer is formed during gastrulation and gives rise to the epithelial lining of the respiratory tract and lungs and also to the digestive tract, thymus, pancreas, and liver [4].

1. The protocol employs hiPSCs at about 1–2 days after splitting as described above. The cells should be at 60%–80% confluency (see **Troubleshooting Problem 2**, Fig. 2A–D)
2. On Day 1, aspirate the mTeSR1/Y-27632 growth medium and add 2 mL or 0.5 mL per well (6- or 24-well plates) of DE differentiation medium (Day 1 medium, Table 1), supplemented with human activin A (100 ng/mL) and the GSK3 $\beta$  inhibitor/Wnt activator CHIR99021 (5  $\mu$ M) to initiate DE differentiation.

**Note:** When two volumes are stated, they apply to 6-well and 24-well plates..

3. On Day 2, 3, and 4, replace the medium with 2 mL or 0.5 mL of the appropriate DE differentiation medium (Day 2, Day 3, Day 4 medium, Table 1), and observe the morphology of the cells. Representative images are shown in Fig. 3A.

**Note:** CHIR99021 should be removed within 24 h of initiating differentiation on Day 1.

4. On Day 5, collect cell sample, extract RNA, and confirm differentiation to DE by qRT-PCR of the DE markers CXCR4, FOXA2, and SOX17 (Fig. 3D). In addition, we also extracted RNA from undifferentiated hiPSC cells to compare the genes for DE markers. Furthermore, DE formation was confirmed by flow cytometry showing >88% population (Fig. S1B).

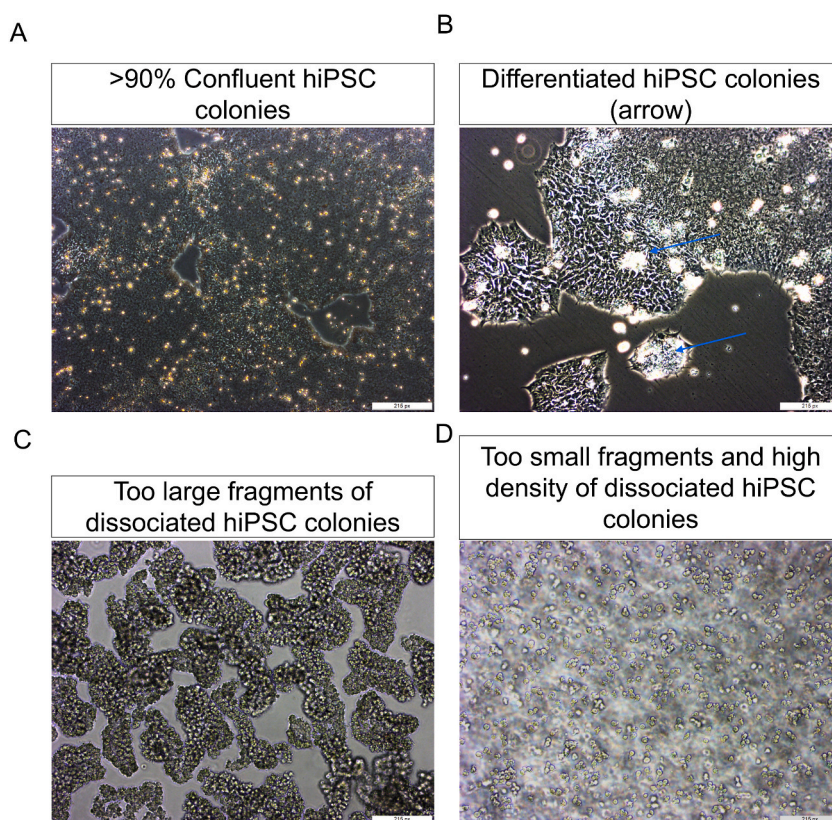


**Fig. 2.** Critical steps and troubleshooting.

(A, B) Representative images of hiPSCs that (A) are at supra optimal confluency (>90%) for dissociation before seeding and (B) have already formed colonies before seeding (blue arrows). Remove differentiated colonies carefully by scraping. Scale bars, 200  $\mu$ m. (C, D) Representative images of hiPSC colonies that are too large (C) and too small and dense (D) after dissociation, both of which are suboptimal for seeding and differentiation. Scale bars, 200  $\mu$ m.

**Table 1**  
Definitive endoderm differentiation medium.

DAY	MEDIUM/SUPPLEMENTS (For 24- and 12-well plate use 0.5 and 1 mL medium/well, respectively, for differentiation)
1	RPMI 1640 + 0% FBS + activin A (100 ng/mL) + CHIR9902, (5 $\mu$ M) + Y27632 (10 $\mu$ M)
2	RPMI 1640 + 0.2% FBS + activin A (100 ng/mL)
3–4	RPMI 1640 + 2% FBS + activin A (100 ng/mL)

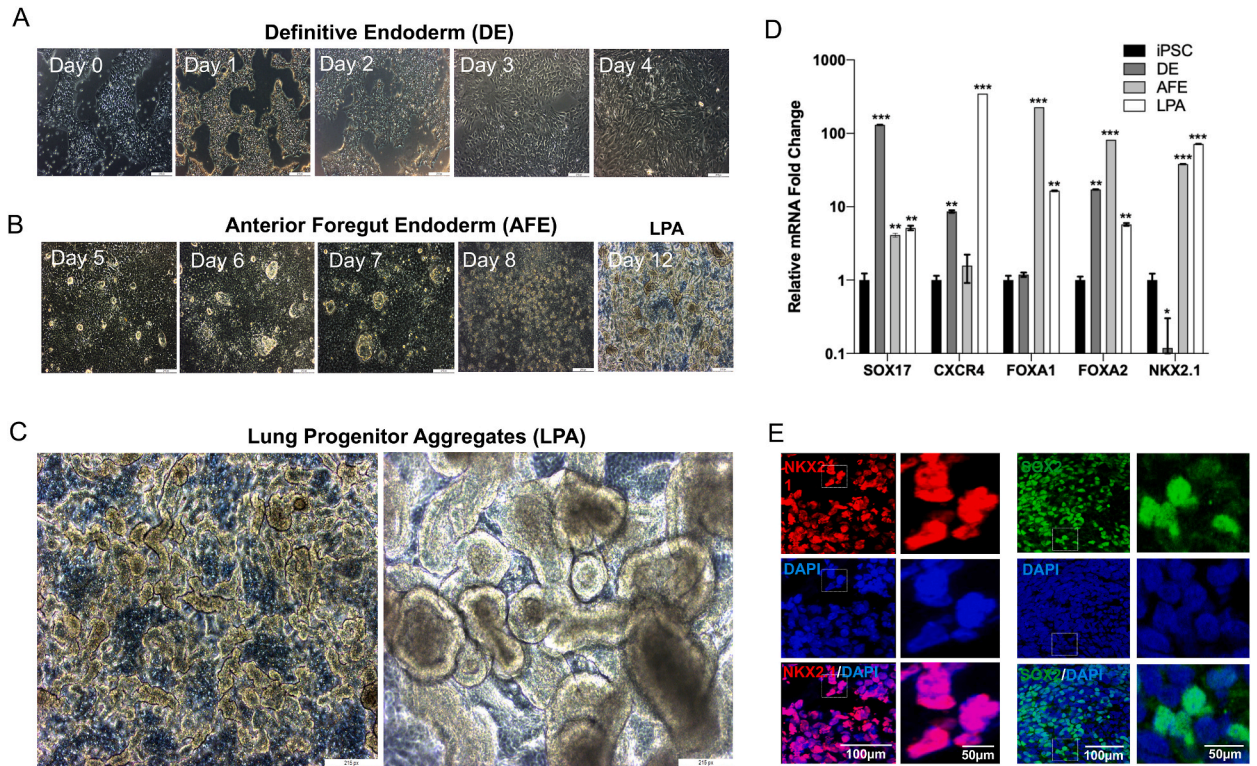


**Fig. 3.** Differentiation of hiPSCs into DE, AFE, and LPAs.

(A, B) Representative light microscopic images showing the typical morphology of hiPSCs upon differentiation to (A) DE and (B) to AFE (Days 5–8) and LPAs (Days 9–12). Scale bars, 200  $\mu$ m. (C) Representative microscopic images showing the lung progenitor aggregate (Day 12) formation. (Scale bar, 200  $\mu$ m left image and 50  $\mu$ m right image) (D) qRT-PCR analysis of expression of genes associated with DE (*SOX17*, *CXCR4*), AFE (*FOXA1*, *FOXA2*), and LPA (*NKX2.1*) in differentiating hiPSCs collected on Days 4, 8, and 12, respectively and also collected undifferentiated hiPSC for qRT-PCR analysis. Data are presented as the mean  $\pm$  SEM ( $n = 3$ ) and are presented as the fold change in mRNA relative to that in hiPSCs. (E) Immunofluorescence staining of LPA-associated proteins (*NKX2.1*, green, *SOX2*, red) on Day 12 of differentiation. Nuclei were stained with 4',6-diamidino-2-phenylindole (DAPI, blue). Scale bars, 100  $\mu$ m.

**Table 2**  
Basal medium.

REAGENT	FINAL CONCENTRATION	AMOUNT for 500 mL
Iscove's Modified Dulbecco's Medium (IMDM)	n/a	375 mL
Ham's F12	n/a	125 mL
N2 supplement	1X	5 mL
B27 supplement (without ATRA)	1X	10 mL
L-Glutamine	2 mM	5 mL
Ascorbic acid	50 $\mu$ g/mL	500 $\mu$ L
Monothioglycerol	0.4 $\mu$ M	500 $\mu$ L
BSA (10% stock)	0.05%	2.5 mL
Penicillin-streptomycin (5000 U/mL)	1X	5 mL

n/a, not applicable.

#### 4. AFE and LPA induction (Days 5–12)

##### 4.1. Timing: 8 days

AFE gives rise to respiratory tissues such as the trachea and lungs [5]. Previous work established that concomitant inhibition of BMP with Noggin and of TGF $\beta$  signaling with SB431542 results in the differentiation of a highly enriched AFE population from DE [6]. At the same time, the growth factor FGF4 and the smoothened agonist (SAG) are added to the culture for differentiation into AFE.

5. On Days 5, 6, 7, and 8, replace the DE differentiation medium with AFE differentiation medium (basal medium [Table 2] supplemented with HEPES buffer 1%, SB431542 10  $\mu$ M, Noggin 200 ng/mL, SAG 1  $\mu$ M, and FGF4 500 ng/mL).
6. Check the cell morphology daily. Representative images are shown in Fig. 3B.
7. On Day 8, collect a cell sample for RNA and immunofluorescence analysis to confirm AFE differentiation by qRT-PCR for expression of FOXA1, FOXA2, and NKX2.1 genes or immunofluorescence microscopy for NKX2.1, showing increase in expression during the transition from DE to AFE (Fig. 3D and E).
8. We also analyzed the expression of posterior markers (CDX2.1, PAX1 and NKX2.5) as a negative control in the same sample used in step 7 and their expression is significantly low as compared to anterior markers (Fig. S1A).
9. On Days 9, 10, 11, and 12, replace the AFE differentiation medium with LPA medium (AFE differentiation medium supplemented with BMP4 - 10 ng/mL, CHIR99021 - 3  $\mu$ M, and ATRA - 0.1  $\mu$ M). CHIR99021 activates Wnt-signaling by binding secreted Wnt-protein to its receptor and extremely potent glycogen synthase kinase (GSK) 3 inhibitor, inhibiting both GSK3 $\beta$  and GSK3 $\alpha$ . Retinoic acid signaling play critical role in balancing lung epithelial progenitor cell growth and differentiation [7] (Ng-Blichfeldt et al., 2018). Prior studies provide evidence that Wnt + BMP signaling (in the presence of RA) is necessary to specify lung progenitors from AFE, whereas FGF and BMP signaling promotes specification to thyroid [8–10], thus we added the CHIR99021, BMP4 and ATRA to specify the AFE into lung progenitors.
10. Monitor the cell morphology daily between Days 8 and 12. Representative images are shown in Fig. 3B and C.
11. On Day 12, collect a cell sample for RNA extraction and immunofluorescence analysis and confirm LPA formation by qRT-PCR and immunofluorescence microscopy analysis of expression of SOX2 and NKX2.1, which are highly expressed in LPAs (Fig. 3C–E and S1A).

#### 5. Formation of 3D LORGs and re-embedding in matrigel (Day 12–60)

##### 5.1. Timing: ~48 days

In the next steps of the protocol, LPAs are mixed with Matrigel (Cat No 354234) and allowed to form 3D LORGs, consisting of an airway-like structure with distal and proximal patterning of mesenchymal and alveolar epithelial cells.

12. Thaw GFR-M on ice.
13. Cut the tip off of a P1000 pipette filter tip and gently triturate the LPAs from the Day 12 plates.
14. Transfer the LPA suspension to from each well into separate 1.5 mL tubes and allow to stand at room temperature for 5–10 min for the aggregates to settle. Alternatively, the tubes can be gently centrifuged at 200RPM for about 10 s.

**CRITICAL:** Handle the cell aggregates gently to avoid disrupting and forming a single cell suspension.

15. Remove the medium from the tubes without disturbing the LPA pellet, add 200  $\mu$ L of cold GFR-M avoiding bubbles, and transfer the LPA/Matrigel mixture to Transwell membrane inserts. Alternatively, pipette ~25  $\mu$ L aliquots of the LPA/GFR-M mixture onto squares of sterile parafilm. Place the Transwell inserts or parafilm squares in a 37  $^{\circ}$ C incubator for 20–30 min to allow the LPA-containing GFR-M to solidify.
16. Once Matrigel embedded cells solidify, add the fresh LPA medium in lower chamber of trans well insert or carefully add medium on sterile film to drop the Matrigel aggregate into 24-well plate which float in the medium.

#### 6. CRITICAL: The LPA/GFR-M mixture should contain no more than 10–15 aggregates per 200 $\mu$ L of GFR-M

##### 6.1. CRITICAL: Keep the matrigel cool at all steps preceding the 37 $^{\circ}$ C incubator to avoid solidification

17. On Days 13 and 14, replace the medium with fresh LPA medium/Matrigel.
18. On Day 15, add 1 mL of LORG culture medium (consisting of basal medium, Table 2 supplemented with FGF10 100 ng/mL, FGF7 10 ng/mL, CHIR99021 3  $\mu$ M, EGF 10 ng/mL, and Y-27632 10  $\mu$ M) to the lower chamber of the Transwell and replace the insert. Change the medium every other day from Day 15 to Day 23. If using parafilm based method, then only carefully remove the medium from side of well without disturbing Matrigel aggregate and add fresh medium.
19. On Day 24, replace the medium in the lower chamber with 1 mL LORG branching medium (consisting of basal medium, Table 2 supplemented with FGF10 100 ng/mL, FGF7 10 ng/mL, CHIR99021 3  $\mu$ M, EGF 10 ng/mL, ATRA 50 nM, VEGF/PIGF 10 ng/mL). Change the medium every other day from Day 24 to Day 32.

20. Monitor the cultures for evidence of branching. On Day 33, replace the medium with 1 mL LORG maturation medium (consisting of LORG branching medium supplemented with cAMP 100  $\mu$ M, DEX 50 nM, and IBMX 100  $\mu$ M). Change the medium every other day from Day 33 to Day 40.

**Note:** If LPAs have not differentiated (as indicated by images in Fig. 3B) or cultures show evidence of cell death or the LORG/Matrigel droplet appears to have adhered to the culture well the cells should be re-embedded as described below (before the scheduled 2-week interval, if necessary).

## 7. Passaging and re-embedding of LORGs

### 7.1. Time: 1–2 h

From Day 40 onwards, the LORG cultures are monitored and LORGs are re-embedded in GFR-M every 2 weeks (or earlier if necessary) to continue branching and maturation..

21. If images show poorly differentiated organoid with cellular debris (Fig. 6A), old Matrigel with attached organoid (Fig. 6B) and healthy floating organoids (Fig. 6C), remove the old Matrigel and re-embed organoids in new Matrigel for further culture.
22. Under a dissecting microscope, use a P1000 pipette tip with the tip cut off to gently pick up the LORG/GFR-M droplet and transfer it to a Petri dish. Use a scalpel and 27-gauge needle to gently remove the old Matrigel and undifferentiated cellular

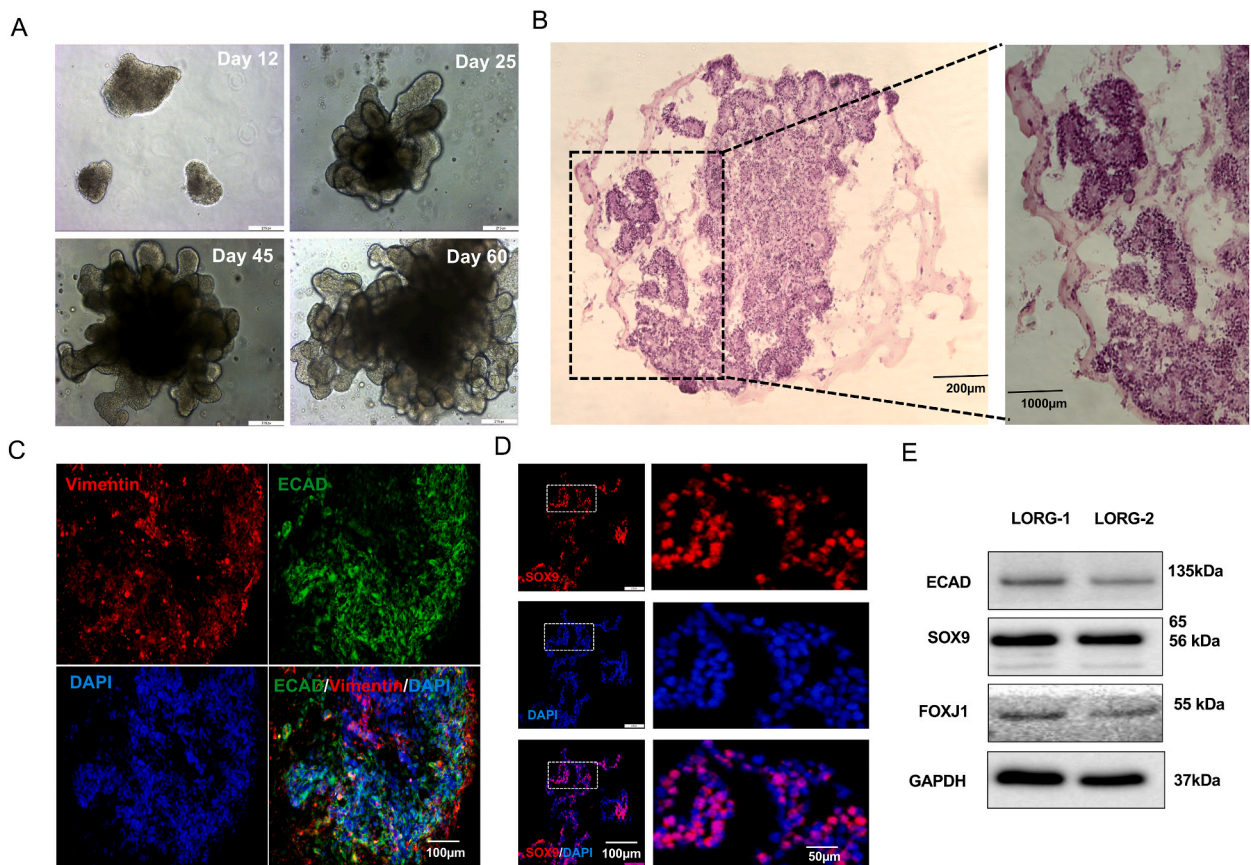


**Fig. 4.** Formation and characterization of 3D LORGs.

(A) Representative phase-contrast images of lung organoids (LORGs) differentiation at indicated days of protocol. Scale bar, 200  $\mu$ m (B) H&E staining of 60D LORG showing alveolar-like morphology. Scale bars, 200  $\mu$ m and 100  $\mu$ m (C) Confocal fluorescence microscopy of a LORG stained at Day 60 for the proximal epithelial marker E-cadherin (ECAD, green) and the mesenchymal cell-type marker vimentin (VIM, red). Nuclei were stained with DAPI (blue). Scale bars, 100  $\mu$ m. (D) Immunofluorescence images of a LORG stained for the distal epithelial marker SOX9 (green). Nuclei were stained with DAPI (blue). Scale bars, 100  $\mu$ m. (E) Immunoblot analysis of LORG lysate showing the intensity of protein level in two individual LORG organoids for epithelial protein (ECAD, band intensities 0.452 and 0.345), ciliated protein (FOXJ1, band intensities 0.231 and 0.211) and lung progenitor markers (SOX9, band intensities 1.45 and 1.323) as compared with internal control GAPDH, band intensities 2.92 and 3.18, n = 2 organoids).

debris. For transwell, we carefully detach all the Matrigel containing organoid with sterile spatula from the wall side of transwell and transfer with 1 mL pipette tip (cut to widen the tip mouth) to a 10 cm Petri-dish containing medium. Under dissecting microscope, carefully remove the old Matrigel and undifferentiated cellular debris with scalpel and 27-gauge needle. Collect the rounded structure containing lung progenitor cells as shown in Fig. 6C. To avoid damage to organoid during removal of old Matrigel, carefully dissect the organoid. In addition, if there is a minor damage, it will not affect the branching and differentiation because they also maintain the lung progenitor cells.

23. Transfer the healthy LORG to a 1.5 mL tube, allow to settle, and remove the remaining medium.
24. Add 200  $\mu$ L of fresh Matrigel to the LORG and use a P200 pipette tip with the tip cut off to gently mix avoiding bubbles. Pipette 40–50  $\mu$ L of the mixture onto sterile parafilm squares and place in a 37 °C incubator for 15–30 min to allow the LORG/Matrigel mixture to solidify.
25. After solidification, carefully transfer the droplets to a 24-well plate (one per well) and add 500  $\mu$ L of LORG maturation medium to each well.

The LORGs can be maintained by repeating steps 20–23 every 2 weeks, but the epithelium is lost over time and cell death increases. Therefore, the LORGs are best used for experiments between ~ Days 50 and 90. LORG showing the branching pattern at different developmental stages (Fig. 4A). We also analyzed intestinal (LGR5, DCAMKL1, BMPR1a) and thyroid (FOXE1, PAX8) markers in lung organoid (Fig. S4B) and we couldn't detect expression of these markers, except low expression of PAX8.

## 8. Immunohistochemical analysis of LORGs

### 8.1. Timing: ~2–3 days

26. Collect the LORGs from culture gently with P1000 pipette tip with the tip cut off, place in a 1.5 mL tube, and wash by adding 1 mL phosphate-buffered saline (PBS). Allow to settle and remove the residual Matrigel by adding 500  $\mu$ L of cell recovery solution and incubating at room temperature for ~30 min.
27. Remove the cell recovery solution and wash with PBS after organoids have settled down (Settling time is around 10min and no need to spin down). Wash the LORGs with PBS and fix by adding 500  $\mu$ L 4% paraformaldehyde and incubating for 1 h at 4 °C.
28. Wash the LORGs again with PBS and dehydrate by adding 500  $\mu$ L 30% sucrose solution followed by incubation overnight at 4 °C. Remove the sucrose, wash the LORGs with PBS and embed in OCT compound or paraffin wax using standard procedures for sectioning Tiwari et al., 2021.
29. Cut 20  $\mu$ m sections from the LORG blocks and perform antigen retrieval by citrate buffer.
30. Using standard tissue immunostaining techniques such as H & E staining and label the LORGs with antibodies against the desired cell markers, including SFTPC, SOX9, SOX2, HTII-280, P63, ECAD and vimentin and immunoblotting (Fig. 4B–E, 5B, 5D, and 7E, Figs. S5–A).

### 8.2. Application of LORGs for modeling viral infection and antiviral drug testing

Note: For additional details about infection and sample processing see Tiwari et al.2021..

LORGs formed using various protocols have been shown to express receptors for various viruses in the proximal and distal airway cell types and are thus useful for investigating not only the mechanism of viral pathogenesis but also the efficacy and mechanisms of action of candidate antiviral drugs [1,11]. We recently employed the LORG protocol described here to investigate SARS-CoV-2 infection and to assess the activity of antiviral drugs [1]. Some of our findings are briefly summarized here to illustrate the utility of the LORG model.

We first asked whether LORGs express the SARS-CoV-2 host co-receptors ACE2 and TMPRSS2. Indeed, qRT-PCR analysis, Western blot analysis, and immunofluorescence staining of LORGs confirmed that the expression of both receptors was equally as robust in Day 60 LORGs as compared to starting hiPSCs (Fig. 7A–C, Figs. S5–B). Moreover, immunofluorescence staining of ACE2 and SFTPC, a marker of SARS-CoV-2 receptor and Alveolar type II (ATII) cells, showed coincident staining, suggesting that SARS-CoV-2 may be able to infect ATII cells in LORGs.

To test this, we infected LORGs with a GFP-tagged SARS-CoV-2 pseudovirus at a multiplicity of infection of 2. GFP fluorescence, indicative of productive SARS-CoV-2 infection, was evident throughout fluorescence imaging of infected LORGs (Fig. 7D).

Moreover, when we infected LORGs with the live SARS-CoV-2 isolate USA-WA1/2020 and co-immunostained for the SARS-CoV-2 nucleocapsid protein (NCP) and HTII-280 a biomarker of lung ATII cells, we observed an overlapping staining pattern (Fig. 7E), consistent with the known ability of SARS-CoV-2 to infect ATII cells in humans [12,13].

Next, to assess whether LORGs might be a useful drug screening model system, we examined the efficacy of several known antiviral compounds, including camostat mesylate, a TMPRSS2 inhibitor [14,15]; 25-hydroxycholesterol (25HC), a naturally occurring antimicrobial product induced by Toll-like receptor engagement [16,17]; and E24, an inhibitor of SARS-CoV-2 protease.

LORGs were preincubated with camostat (10  $\mu$ M) for 2 h and then infected with SARS-CoV-2-luciferase pseudovirus. Two hours later, the virus-containing supernatant was removed, and the cells were incubated for an additional 22 h in camostat-containing medium before the cells were lysed and luciferase activity was measured. As shown in Fig. 7F, camostat efficiently (~2–3-fold) and significantly inhibited SARS-CoV-2 infection of LORGs. Similar experiments with LORGs treated with 5  $\mu$ M 25HC and then infected with SARS-CoV-2-luciferase pseudovirus showed an even more impressive suppression of SARS-CoV-2 infection by 25 HC (Fig. 7G).



Finally, we assessed the effects of treatment with E24 (5  $\mu$ M) on LORG infection with live SARS-CoV-2 isolate USA-WA1/2020. qRT-PCR analysis of infected cells demonstrated significant suppression of SARS-CoV-2 NCP expression in supernatant and cellular RNA, confirming the antiviral activity of E24 (Fig. 7H, I, J).

These data highlight the utility of the LORG model system for investigation of the molecular events underlying respiratory viral infection as well as for drug screening. The LORG model will undoubtedly also prove useful for investigating the cellular and molecular pathways that regulate early lung development and cell fate specification [18–20].

Expected outcomes.

- hiPSC cultures should be 60–80% confluent after 1–2 days of plating before DE induction. During DE induction, daily medium exchange removes dead cells and maintains healthy adherent cells, as indicated by expression of SOX17 and CXCR4 by Day 4 (Fig. 3A, D).
- By Day 7–9 of AFE induction, a heterogenous population of adherent cells appears with some floating spheroids, which were termed “foregut spheroids” by Miller et al., 2019 to differentiate them from the loosely adherent AFE aggregates (i.e., LPAs) that appear around Day 12 (Fig. 3B and C).
- Analysis of gene expression should confirm the presence of AFE expressing FOXA1, FOXA2, and NKX2.1 by Day 8, and of LPAs expressing high levels of SOX2 and NKX2.1 by Day 12 (Fig. 3D–E and S1A).
- The AFE/LPA cultures contain both lung (NKX2.1) and gastric (SOX2+) progenitor cells (Fig. 3E), as is seen during early embryonic development in humans.

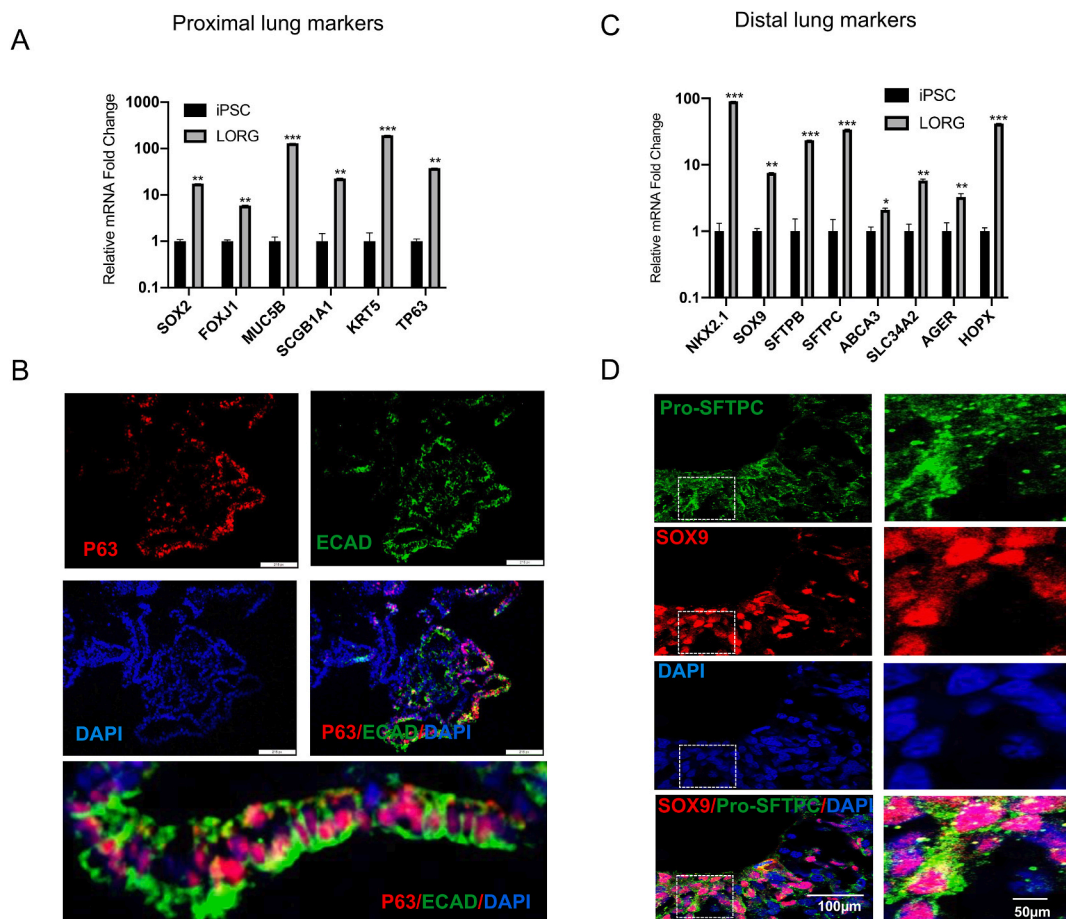


**Fig. 5.** Expression of proximal and distal lung markers in LORGs.

(A) qRT-PCR analysis of the proximal lung genes *SOX2*, *FOXJ1*, *MUC5B*, *SCGB1A1*, *KRT5*, and *TP63* in hiPSCs or in LORGs collected on Day 60. Data are the mean  $\pm$  SEM ( $n = 3$ ) and are presented as the fold change in mRNA level relative to that in hiPSCs. \* $P < 0.05$ , \*\* $P < 0.01$ , \*\*\* $P < 0.001$ . (B) Immunofluorescence confocal microscopy of a LORG stained for the basal cell marker P63 (red) and the epithelial marker E-cadherin (ECAD, green). Nuclei were stained with DAPI (blue). Scale bars, 100  $\mu$ m. (C) qRT-PCR analysis of the distal lung genes *NKX2.1*, *SOX9*, *SFTPB*, *SFTPC*, *ABCA3*, *SLC34A2*, *AGER*, and *HOPX* in hiPSCs or in LORGs collected on Day 60. Data are the mean  $\pm$  SEM ( $n = 3$ ) and are presented as the fold change in mRNA level relative to that in hiPSCs. \* $P < 0.05$ , \*\* $P < 0.01$ , \*\*\* $P < 0.001$ . (D) Immunofluorescence confocal microscopy of a LORG stained for the distal progenitor cell marker SOX9 (red) and ATII cell-type marker Pro-SFTPC (green). Nuclei were stained with DAPI (blue). Scale bars, 100  $\mu$ m.

- Earlier protocols for differentiation of LORGs from AFE/LPAs (e.g., sorting of NKX2.1+ cells) resulted in enrichment of ATII-like cells but lacked mesenchymal cells. Thus, our protocol improves upon these methods by yielding LORGs that contain both epithelial and mesenchymal cell populations (Fig. 4A–D, E).
- LORGs express proximal lung markers (SOX2, FOXJ1, MUC5B, KRT5, and TP63) and distal lung markers (SOX9, SFTPB, SFTPC, AGER, ABCA3, and HOPX) (Fig. 5A–D). Additionally, LORGs show strong expression of SOX9 (Fig. 5C, D), a transcription factor required for distal lung epithelial cell formation.
- As noted above, the LORGs produced by this protocol express ACE2 and TMPRSS2 receptors and can be infected with SARS-CoV-2, reminiscent of the human lung (Fig. 7A–C), particularly the ATII cells (Fig. 7E).
- Finally, the LORG model system has utility for antiviral drug candidate testing, as shown here for camostat, 25HC, and E24 (Fig. 7F–J).

### 8.3. Advantages and disadvantages

Our aim of this protocol is to create whole lung organoid model containing both bronchial/proximal and alveolar/distal cells (Fig. 5A–D) for better modeling the lung development and infection mechanisms. Advantages and disadvantages of the protocol is outlined below.

1. Current protocol is based on human iPSC derived cells which is easy to get and culture while obtaining bronchial tissue is difficult from patient due to ethical concern.
2. Current protocol showing complete lung organoids formation which express markers for both bronchial airway cells (SOX2, FOXJ1, KRT5 and TP63) and alveolar cells (SOX9, SFTPC) (Fig. 5A–D), while bronchial epithelial cell culture not showing distal organoid markers.
3. Bronchial epithelial cell culture in interface air-liquid condition has more physiological relevance due to mimicking similar to human bronchial airway structure compared to current protocol. We could adapt the current protocol to culture as air-liquid condition during trans well culture in future.
4. In addition, current protocol shows branching morphogenesis and lung mesenchymal cells. Further by re-embedding, we can culture for longer duration without the loss of cellular integrity, while tissue obtained bronchial epithelial cells in interface air-liquid conditions for longer culture is difficult. (Included in text at page 11)

### 8.4. Quantification and statistical analysis (optional)

The data presented here are expressed as the means  $\pm$  standard error (SEM) of three independent biological replicates. Differences between group means was analyzed with by unpaired two-tailed Student's *t*-test. A P value  $< 0.05$  was considered significant.

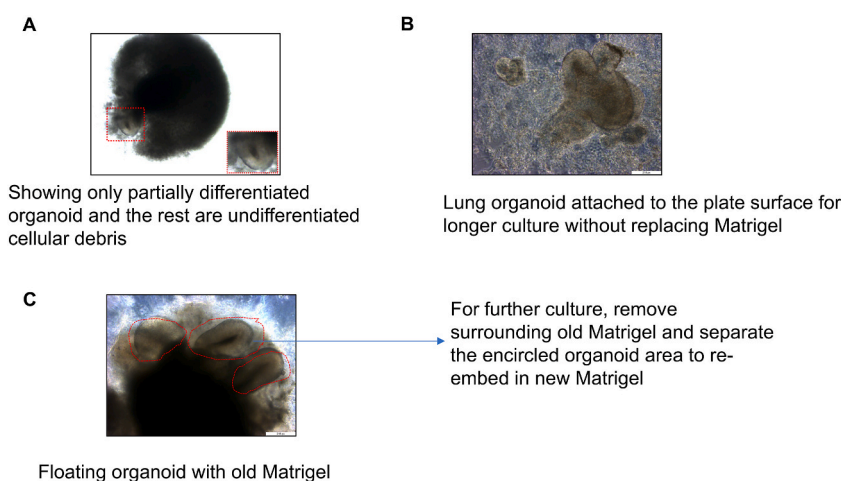


**Fig. 6.** Passaging and re-embedding of organoids.

(A) Representative phase contrast image showing failed Lung organoid differentiation and cell death. Scale bars, 200  $\mu$ m (B) Microscopic image showing lung organoid attached to plate surface because of longer culture without changing the Matrigel. Scale bars, 200  $\mu$ m (C) Representative phase contrast image showing well differentiated Lung organoid that requires replacing old Matrigel and passaging the organoid into new Matrigel. Scale bars, 200  $\mu$ m.

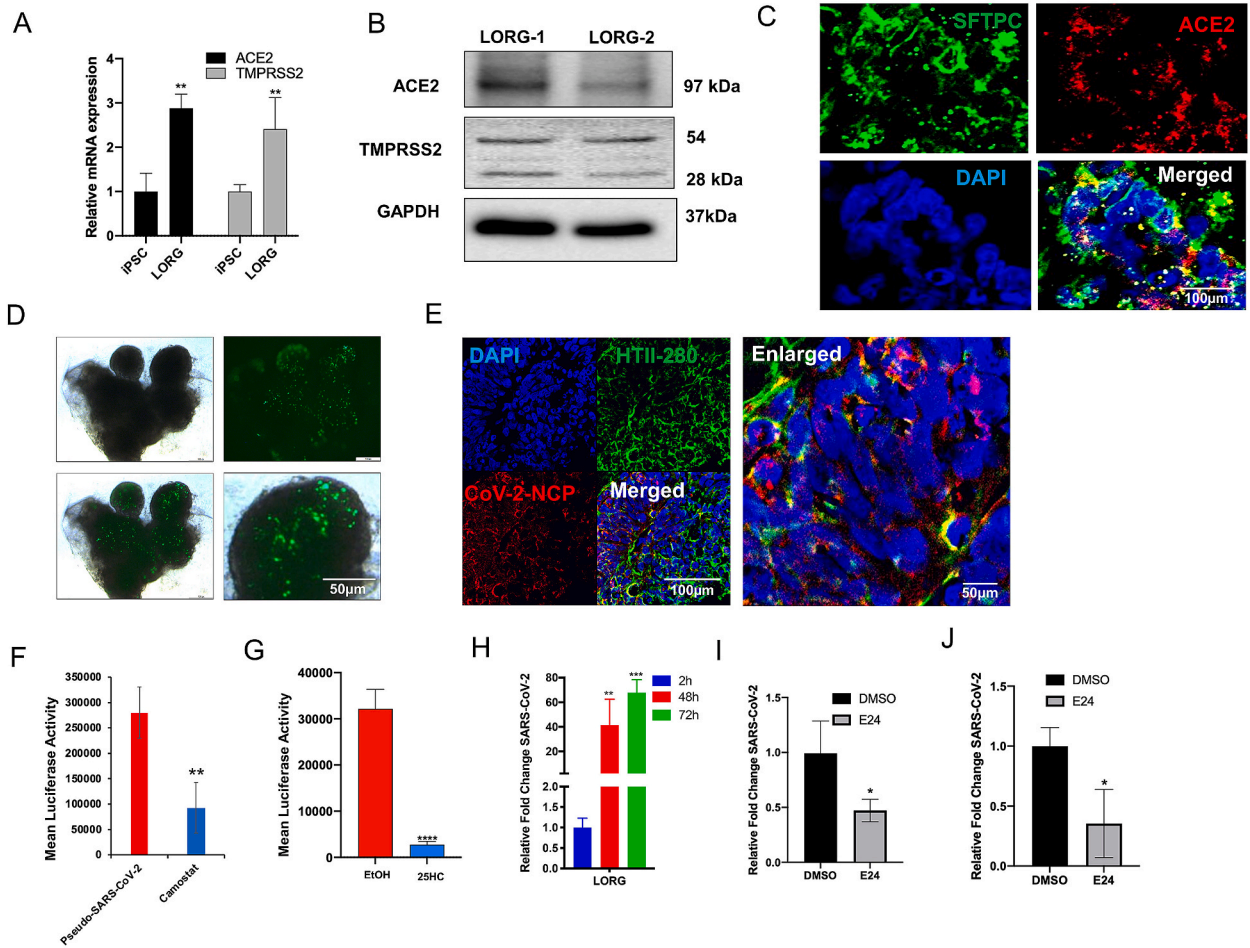


**Fig. 7.** LORGs as a model system for investigation of viral infection and screening of antiviral drugs. (A) qRT-PCR analysis of the SARS-CoV-2 receptors *ACE2* and *TMPRSS2* in hiPSCs or in LORGs collected on Day 60. Data are the mean  $\pm$  SEM ( $n = 3$ ) and are presented as the fold change in mRNA level relative to that in hiPSCs. \* $P < 0.05$ , \*\* $P < 0.01$ . (B) Immunoblot analysis of *ACE2* (band intensities 0.321, 0.245) and *TMPRSS2* (band intensities 0.421 and 0.398) protein expression in two independent LORGs collected on Day 60. GAPDH (band intensities 2.92 and 3.18) was probed as a loading control. (C) Immunofluorescence staining of LORGs for *ACE2* (red) and the ATII cell-type marker SFTPC (green). Nuclei were stained with DAPI (blue). Scale bars, 100  $\mu$ m (D) Phase contrast (upper left) and fluorescence microscopy images of a LORG at 24 h after infection with a GFP-tagged SARS-CoV-2 pseudovirus (green) at a MOI of 2. Upper right and lower left panels show GFP signals of pseudovirus and merged GFP signals with organoid, respectively. Lower right panel shows an enlarged portion of the lower left panel. Scale bars, 200  $\mu$ m, except lower right, 50  $\mu$ m. (E) Immunofluorescence staining of a LORG for the SARS-CoV-2 nucleocapsid protein (CoV-2-NCP, red) and the lung ATII cell marker HT280 (green) at 96 h after infection with SARS-CoV-2 USA-WA1/2020 virus at a MOI of 2. Nuclei were stained with DAPI. Scale bars, 100  $\mu$ m. Magnification of enlarged merged image = 50  $\mu$ m. (F) Luciferase activity in Day 60 LORGs pretreated with vehicle (red) or the *TMPRSS2* inhibitor camostat mesylate (10  $\mu$ M, blue) for 2 h, infected with SARS-CoV-2-luciferase pseudovirus for 2 h, and then washed and incubated in camostat-containing medium for an additional 22 h. Luciferase activity was measured at 24 h post-infection. Data are shown as the mean  $\pm$  SEM of  $n = 3$  independently cultured LORGs. \*\* $P < 0.01$ . (G) Luciferase activity in Day 60 LORGs pretreated with ethanol or 25-hydroxy cholesterol (25HC, 5  $\mu$ M) for 16 h, infected with SARS-CoV-2-luciferase pseudovirus at MOI of 0.1 for 2 h, and then washed and incubated in 25HC-containing medium for an additional 22 h. Luciferase activity was measured at 24 h post-infection. Data are shown as the mean  $\pm$  SEM of 3 LORGs. \*\*\*\* $P < 0.0001$ . Data are taken from Fig. 5D in (Wang et al., 2020). (H) LORGs were infected with SARS-CoV-2 USA-WA1/2020 virus at MOI = 2 for 2, 48 and 72 h and after respective post-infection, qRT-PCR showing increased replication of SARS-CoV-2.  $N = 3$ , mean  $\pm$  SEM \*\* $P < 0.01$ , \*\*\* $P < 0.001$  by Student's t-test (taken from Fig. 2D, Tiwari et al., 2021) (I, J) qRT-PCR analysis of SARS-CoV-2 nucleocapsid mRNA expression in LORGs pretreated with the protease inhibitor E24 (5  $\mu$ M) for 2 h, infected with SARS-CoV-2 USA-WA1/2020 at a MOI of 1 for 2 h, and then washed and incubated in E24-containing medium for an additional 48 h. Data are shown as the mean  $\pm$  SEM ( $n = 3$  LORGs) and are presented as the fold change in mRNA level relative to that in DMSO-treated LORGs. \* $P < 0.05$ .

### 8.5. Limitations

- In this protocol, we have not established the transplantation of these lung organoids into mice for further understanding the vascularization and mature cellular architecture ...

- We have tested this protocol using only two hiPSC lines (iPSC-11 and iPSC-12).
- The LORGs do not appear to contain pulmonary vasculature.
- The LORGs are not terminally differentiated.
- The LORGs contain random branching and the pattern of mesenchyme is undefined. (Mesenchymal cell type determining the shape and size of the lung, so here mentioned the pattern of mesenchyme)

## 9. Troubleshooting

### 9.1. Problem 1

Compromised pluripotency state of hiPSCs during culture.

### 9.2. Potential solution

Remove differentiated cells by scraping and colonies should be well separated from each other as shown in [Fig. 1A and B and 2A-B](#).

### 9.3. Problem 2

Failure of DE to form AFE/LPAs.

### 9.4. Potential solution

- Ensure that hiPSCs are used at a low passage number and do not contain differentiated colonies ([Fig. 2A and B](#)).
- The hiPSC seeding density is important and should be optimized ([Fig. 2C and D](#)).
- Special attention should be paid to ensuring that growth factors are stored under optimal conditions.

### 9.5. Problem 3

Many LPAs fail to differentiate into LORGs and cell death is extensive.

### 9.6. Potential solution

Remove the viable LORGs and re-embed them in fresh LORG medium/GFR-M to rescue and continue the culture.

## 10. Problem 4

LORGs may adhere to the plates and fail to grow properly.

### 10.1. Potential solution

- Re-embed the LORGs in fresh LORG medium/GFR-M.
- Handle GFR-M carefully and place at 4 °C only for the indicates times.

## Resource availability

We require three subheadings in this section (lead contact, materials availability, and data and code availability). The guidelines include instructions and examples.

### Lead contact

Further information and requests for resources and reagents should be directed to and will be fulfilled by the lead contact Tariq M. Rana ([trana@health.ucsd.edu](mailto:trana@health.ucsd.edu)).

### Materials availability

This study did not create new unique materials or chemicals.

### Data and code availability

This study did not generate any unique datasets or code.

## Funding details

This work was supported in part by institutional funds and grants from the National Institutes of Health (CA177322, DA039562, DA049524, and AI125103).

## Author contributions

S.K.T. designed and performed experiments, analyzed the data, and wrote the manuscript. T.M.R. conceived the overall project and experimental design, participated in data analysis and interpretation, and co-wrote the manuscript.

## Declaration of competing interest

The authors declare that they have no known competing financial interests or personal relationships that could have appeared to influence the work reported in this paper.

## Acknowledgments

We thank Dr. F. Furnari for the hiPSC lines and members of the Rana lab for helpful discussions and advice. The following reagent was deposited by the Centers for Disease Control and Prevention and obtained through BEI Resources, NIAID, NIH: SARS-Related Coronavirus 2, Isolate USA-WA1/2020, NR-52281.

## Appendix A. Supplementary data

Supplementary data to this article can be found online at <https://doi.org/10.1016/j.heliyon.2023.e19601>.

## References

- [1] S.K. Tiwari, et al., Revealing tissue-specific SARS-CoV-2 infection and host responses using human stem cell-derived lung and cerebral organoids, *Stem Cell Rep.* 16 (2021) 437–445.
- [2] S.L. Leibel, et al., Reversal of surfactant protein B deficiency in patient specific human induced pluripotent stem cell derived lung organoids by gene therapy, *Sci. Rep.* 9 (2019), 13450.
- [3] A.J. Miller, et al., Generation of lung organoids from human pluripotent stem cells in vitro, *Nat. Protoc.* 14 (2019) 518–540.
- [4] K.A. D'Amour, et al., Efficient differentiation of human embryonic stem cells to definitive endoderm, *Nat. Biotechnol.* 23 (2005) 1534–1541.
- [5] A.M. Zorn, J.M. Wells, Vertebrate endoderm development and organ formation, *Annu. Rev. Cell Dev. Biol.* 25 (2009) 221–251.
- [6] M.D. Green, et al., Generation of anterior foregut endoderm from human embryonic and induced pluripotent stem cells, *Nat. Biotechnol.* 29 (2011) 267–272.
- [7] J.-P. Ng-Blichfeldt, A. Schrik, R. Kortekaas, J.A. Noordhoek, I.H. Heijink, P.S. Hiemstra, J. Stolk, M. Königshoff, R. Gosens, Retinoic acid signaling balances adult distal lung epithelial progenitor cell growth and differentiation, *EBioMedicine* 36 (2018) 461–474.
- [8] M. Serra, et al., Pluripotent stem cell differentiation reveals distinct developmental pathways regulating lung- versus thyroid-lineage specification, *Development* 144 (2017) 3879–3893.
- [9] B. Varghese, Z. Ling, X. Ren, Reconstructing the pulmonary niche with stem cells: a lung story, *Stem Cell Res. Ther.* 13 (2022) 161.
- [10] W. Yang, et al., Human lung organoid: models for respiratory biology and diseases, *Dev. Biol.* 494 (2023) 26–34.
- [11] Y. Han, et al., Identification of SARS-CoV-2 inhibitors using lung and colonic organoids, *Nature* 589 (2021) 270–275.
- [12] A.A. Salahudeen, et al., Progenitor identification and SARS-CoV-2 infection in human distal lung organoids, *Nature* 588 (2020) 670–675.
- [13] H. Katsura, et al., Human lung stem cell-based alveolospheres provide insights into SARS-CoV-2-mediated interferon responses and pneumocyte dysfunction, *Cell Stem Cell* 27 (2020) 890–904 e8.
- [14] M. Hoffmann, et al., SARS-CoV-2 variants B.1.351 and P.1 escape from neutralizing antibodies, *Cell* 184 (2021) 2384–2393 e12.
- [15] M. Hoffmann, et al., Camostat mesylate inhibits SARS-CoV-2 activation by TMPRSS2-related proteases and its metabolite GBPA exerts antiviral activity, *EBioMedicine* 65 (2021), 103255.
- [16] R. Zang, et al., Cholesterol 25-hydroxylase suppresses SARS-CoV-2 replication by blocking membrane fusion, *Proc. Natl. Acad. Sci. U. S. A.* 117 (2020) 32105–32113.
- [17] S. Wang, et al., Cholesterol 25-Hydroxylase inhibits SARS-CoV-2 and other coronaviruses by depleting membrane cholesterol, *EMBO J.* 39 (2020), e106057.
- [18] A. Fatehullah, S.H. Tan, N. Barker, Organoids as an in vitro model of human development and disease, *Nat. Cell Biol.* 18 (2016) 246–254.
- [19] M.Z. Nikolic, E.L. Rawlins, Lung organoids and their use to study cell-cell interaction, *Curr Pathobiol Rep* 5 (2017) 223–231.
- [20] D. McCulley, M. Wienhold, X. Sun, The pulmonary mesenchyme directs lung development, *Curr. Opin. Genet. Dev.* 32 (2015) 98–105.